Title

Identification of three novel Toxoplasma gondii rhoptry proteins

Journal

International Journal for Parasitology, 44(2)

ISSN

0020-7519

Authors

Camejo, Ana

Gold, Daniel A

Lu, Diana

et al.

Publication Date

2014-02-01

DOI

10.1016/j.ijpara.2013.08.002

Peer reviewed

International Journal for Parasitology 44 (2014) 147–160

Contents lists available at ScienceDirect

International Journal for Parasitology

journal homepage: www.elsevier.com/locate/ijpara

Identification of three novel *Toxoplasma gondii* rhoptry proteins

Ana Camejo [a], Daniel A. Gold [a], Diana Lu [a], Kiva McFetridge [b], Lindsay Julien [a], Ninghan Yang [a], Kirk D.C. Jensen [a], Jeroen P.J. Saeij [a,*]

[a] Department of Biology, Massachusetts Institute of Technology, Cambridge, MA 02139, USA
[b] Department of Biochemistry, Texas State University, San Marcos, TX 78666, USA

ARTICLE INFO

Article history:
Received 4 April 2013
Received in revised form 6 August 2013
Accepted 6 August 2013
Available online 24 September 2013

Keywords:
Toxoplasma gondii
Rhoptry
Rhoptry neck
Host–pathogen interaction

ABSTRACT

The rhoptries are key secretory organelles from apicomplexan parasites that contain proteins involved in invasion and modulation of the host cell. Some rhoptry proteins are restricted to the posterior bulb (ROPs) and others to the anterior neck (RONs). As many rhoptry proteins have been shown to be key players in *Toxoplasma* invasion and virulence, it is important to identify, understand and characterise the biological function of the components of the rhoptries. In this report, we identified putative novel rhoptry genes by identifying *Toxoplasma* genes with similar cyclical expression profiles as known rhoptry protein encoding genes. Using this approach we identified two new rhoptry bulb (ROP47 and ROP48) and one new rhoptry neck protein (RON12). ROP47 is secreted and traffics to the host cell nucleus, RON12 was not detected at the moving junction during invasion. Deletion of ROP47 or ROP48 in a type II strain did not show major influence in in vitro growth or virulence in mice.

1. Introduction

Toxoplasma gondii is a highly successful parasite infecting approximately 30% of people worldwide and is the second largest cause of death due to foodborne illness in the United States (Scallan et al., 2011). Toxoplasmosis can be fatal in the unborn fetus and in immunosuppressed individuals if the disease is not recognised and treated early, in contrast to immunocompetent patients in whom it is mainly self-limited (Montoya and Liesenfeld, 2004; Scallan et al., 2011).

Toxoplasma resides within a non-fusogenic parasitophorous vacuole and has three apical secretory organelles: the dense granules, micronemes and rhoptries. Rhoptries are club-shaped organelles divided into two distinct compartments, the posterior bulb and the more anterior duct (neck) through which rhoptry proteins are secreted. Proteins derived from the rhoptry secretory organelles are crucial for the invasion and survival of apicomplexan parasites within host cells and thus rhoptry protein targeting is a vital process for *Toxoplasma*. Some rhoptry proteins are restricted to the bulb (ROPs) and others to the neck (RONs). The role of rhoptries in the invasion process, virulence and/or host cell modulation has been well documented, although the molecular mechanisms remain only partially understood. RONs 2, 4, 5 and 8 have been shown to be involved in parasite invasion of the host cell (Besteiro et al., 2009; Straub et al., 2009); ROP16 activates the transcription factors STAT3 and STAT6 (Saeij et al., 2007; Yamamoto et al., 2009; Ong et al., 2010); ROP38 downregulates Mitogen Activated Protein Kinase (MAPK) pathway activation (Peixoto et al., 2010); and ROP5 and ROP18 act jointly to block immunity-related GTPase (IRG) mediated clearance of the parasite by the host cell (Behnke et al., 2012; Fleckenstein et al., 2012; Niedelman et al., 2012). Once rhoptry proteins are secreted into the host cell cytosol they traffic to distinct cellular destinations. For example, ROP16 and the rhoptry protein phosphatase 2 C (PP2C-hn) carry a nuclear localisation signal (NLS), which mediates their trafficking to the host nucleus (Gilbert et al., 2007; Saeij et al., 2007), ROP5 and ROP18, following secretion into the host cell, traffic back to the outside of the parasitophorous membrane vacuole (PVM) via an arginine-rich amphipathic helix domain that is essential for this localisation (Reese and Boothroyd, 2009; Fentress et al., 2012). Other rhoptry proteins, such as Toxofilin, remain in the host cell cytosol upon secretion (Lodoen et al., 2010).

Rhoptry proteins contain a classic eukaryotic signal peptide for entrance into the secretory pathway and are trafficked from the endoplasmic reticulum through the Golgi by a conserved pathway before being packaged into the apically located secretory organelles (Sadak et al., 1988; Bradley and Boothroyd, 1999; Bradley et al., 2004; Carey et al., 2004; Hajj et al., 2006b, 2007; Turetzky et al., 2010). N-terminal pro-domains have been implicated in rhoptry protein sorting and indeed several rhoptry proteins exhibit N-terminal processing. However, the failure to remove the pro-domain does not seem to disrupt targeting (Bradley et al., 2002; Miller et al., 2003; Turetzky et al., 2010). Other rhoptry proteins do not appear to be processed and the mechanism by which they

* Corresponding author. Address: 77 Massachusetts Ave, Building 68-270b, Cambridge, MA 02139, USA. Tel.: +1 617 324 5330; fax: +1 617 253 9810.
E-mail address: jsaeij@mit.edu (J.P.J. Saeij).

0020-7519/$36.00
http://dx.doi.org/10.1016/j.ijpara.2013.08.002

are targeted to the rhoptries is unknown. Additionally, any soluble protein recombinantly fused to a signal peptide is delivered to the dense granules by default (Joiner and Roos, 2002). Therefore, motifs that mediate trafficking of proteins to the rhoptry organelles are insufficiently defined, or insufficiently specific, to allow genome-wide identification of rhoptry proteins.

Proteomic and genomic approaches have been widely used to identify the contents of the rhoptries of apicomplexan parasites (Hoppe et al., 2000; Bradley et al., 2005; Peixoto et al., 2010; Marugán-Hernández et al., 2011; Reid et al., 2012; Oakes et al., 2013). A proteomic study of *Toxoplasma* rhoptry contents led to the identification of 38 rhoptry proteins (Bradley et al., 2005). Twenty of these proteins were shown to localise to the rhoptry organelles, 11 to the rhoptry bulb and nine to the rhoptry neck (Bradley et al., 2005; Taylor et al., 2006; Gilbert et al., 2007; Proellocks et al., 2009; Straub et al., 2009; Peixoto et al., 2010; Lamarque et al., 2012). As expected, several previously known rhoptry proteins were readily detected in this proteomic analysis. However, TgNHE2 and TgSUB2, previously characterised as rhoptry proteins, were missed. The absence of these known rhoptry proteins is likely due to limitations of the technique, such as size cut-off or low amounts of protein.

Because several rhoptry proteins, such as the aforementioned ROP5, ROP16, ROP18 and ROP38, contain kinase-like domains (Hajj et al., 2006a; Peixoto et al., 2010), another study exploited a phylogenomic approach to characterise the *Toxoplasma* kinome, defining a 44-member family of kinase-like rhoptry proteins based on sequence similarities, including all previously reported kinase-like rhoptry proteins (Peixoto et al., 2010). To evaluate the accuracy of these predictions, nine of the identified kinase-like rhoptry proteins were confirmed to localise to the rhoptries, whereas two (ROP21 and ROP22) did not but were still annotated as rhoptry proteins. Surprisingly, the overlap between these two studies is relatively small, with only 11 genes found in common, which emphasizes the complementarity of different methodologies and the likelihood that there are still rhoptry proteins yet to be identified.

Previous characterisation of the cell cycle transcriptome of *Toxoplasma* covering 12 h post-synchronisation and nearly two tachyzoite replication cycles showed that the mRNA levels of genes encoding for proteins secreted from the rhoptry organelles display a cyclical expression profile, reaching peak levels in late S phase/early mitosis followed by a rapid and dramatic decline of these transcripts in early G1, before peaking again in the next S phase (Behnke et al., 2010). Inner membrane complex (IMC) mRNAs presented a very similar cyclical expression profile. Microneme mRNAs were offset by 1–2 h from rhoptry mRNAs and defined a distinct temporal class. By contrast, dense granule mRNAs largely were not regulated in the tachyzoite cell cycle.

Here we combined in silico and in vivo methods to identify novel rhoptry proteins likely to be involved in parasite modulation of host cells and found two novel rhoptry bulb proteins and one novel rhoptry neck protein.

2. Materials and methods

2.1. Parasites and cell lines

Parasites were maintained in vitro by serial passage on monolayers of human foreskin fibroblasts (HFFs) at 37 °C in 5% CO_2. HFFs were grown in DMEM supplemented with 10% FBS. C57BL6/J mouse embryonic fibroblasts (MEFs) were a gift from A. Sinai (University of Kentucky College of Medicine, Lexington, KY, USA) and were grown in HFF media supplemented with 10 mM HEPES, 1 mM sodium pyruvate and 1× non-essential amino acids.

2.2. Identification of candidate genes

For identification of new rhoptry protein coding genes, cell cycle transcriptome data of the *T. gondii* during synchronised growth in human foreskin fibroblasts (HFFs) deposited at Gene Expression Omnibus (GEO) with accession number GSE19092 were used (Behnke et al., 2010). The data were normalised using Robust Multi Array (RMA) algorithm using Affymetrix Expression Console Software version 1.3.1, and all background values less than 6.5 were set to 6.5. Genes with an expression value of less than 6.5 in 12 or more samples where removed from the analysis. K-means clustering of each duplicated sample (time-point) was performed using the default distance metric (Pearson correlation) and a maximum number of 50, 45, 40, 35, 30, 25, 20, 12 and 10 clusters in Multiple Array Viewer 4.6. The cluster with the largest number of previously annotated rhoptry proteins was chosen for further analysis. The candidate genes were chosen using the following criteria: (i) contained a predicted signal peptide, (ii) had unannotated function and (iii) unknown subcellular localisation.

2.3. Gene tagging

Genomic sequences were obtained from the ToxoDB database (Version 8.0, ToxoDB.org) (Kissinger et al., 2003). For endogenous gene tagging (Huynh and Carruthers, 2009), primers were designed to amplify 1–3 kb of the predicted 3′ ends of genes. For heterologous expression of ROP47, the coding regions of TGME49_261740, together with putative promoter (~1500 bp upstream of ATG start codon) were amplified by PCR. All forward primers contained the 5′-CACC-3′ sequence required to perform directional TOPO cloning in pENTR/D-TOPO (Invitrogen, USA) and all reverse primers contained the hemagglutinin (HA) tag sequence followed by a stop codon (Table 1). HA-tagged sequences were cloned in vector pTKOatt by Gateway Recombination Cloning Technology (Invitrogen, USA). For endogenous gene tagging, the resulting vectors were linearised using a restriction enzyme with a unique restriction site within the cloned fragment. Linearised vector was transfected into RHΔ*hxgprtΔku80* (a gift from V. Carruthers, University of Michigan, Ann Arbor, MI, USA) parasites by electroporation. For heterologous expression of ROP47, vector was not linearised and was transfected into RHΔ*hxgprt*. Electroporation was done in a 2 mm cuvette (Bio-Rad Laboratories, USA) with 2 mM ATP (MP Biomedicals, USA) and 5 mM glutathione (EMD, Germany) in a Gene Pulser Xcell (Bio-Rad Laboratories), with the following settings: 25 μFD, 1.25 kV, $\infty\Omega$. Stable integrants were selected in media with 50 μg/ml of mycophenolic acid (Axxora, USA) and 50 μg/ml of xanthine (Alfa Aesar, USA) and cloned by limiting dilution. The correct tagging of each gene was confirmed by PCR, using a primer upstream of the plasmid integration site and a primer specific for the HA tag and/or by immunofluorescence (IF) analysis.

2.4. IF analysis

Parasites were allowed to invade cells on coverslips and incubated for 16–24 h. The cells were then fixed with 3% (vol/vol) formaldehyde in PBS for 20 min at room temperature and blocked in PBS with 3% (wt/vol) BSA and 5% (vol/vol) goat serum. Coverslips were incubated with primary antibody for 1 h at room temperature or overnight at 4 °C, and fluorescent secondary antibodies and Hoechst dye were used for antigen and DNA visualisation, respectively. Coverslips were mounted on a glass slide with Vectashield (Vector Laboratories, USA), and photographs were taken using NIS-Elements software (Nikon, Japan) and a digital camera (CoolSNAP EZ; Roper Industries, USA) connected to an inverted fluorescence microscope (model eclipse Ti–S; Nikon). To determine seroconversion, peripheral blood serum was used as a primary

Table 1
Primers used in this study.

Gene ID	Forward primer		Reverse primer	
Primers used for gene tagging (5′–3′)				
TGME49_201860	CACCTCGCGACCACCTGCGTTTTGA		TTACGCGTAGTCCGGGACGTCGTACGGGTAGAGTTCAGCGAAAGCACCTGC	
TGME49_210370	CACCACAGCCCGTTACGTCTTGCGAC		TTACGCGTAGTCCGGGACGTCGTACGGGTAAACGGAGGGAAGAAACGGGG	
TGME49_218270	CACCGGCTGGAGATTTTTCCCCGGAACT		TTACGCGTAGTCCGGGACGTCGTACGGGTAAGCCGGACTTGCAGAAGGCAC	
TGME49_225160	CACCCCATGCTTCTGTTCGCAGAAAT		TTACGCGTAGTCCGGGACGTCGTACGGGTATGAATCCTTGAAACTGCGAATC	
TGME49_232020	CACCTGGCTCTCCAGCCGCGGCGATT		TTACGCGTAGTCCGGGACGTCGTACGGGTATCGTCGCCGGCGCCTTCCGC	
TGME49_237180	CACCAGAAACCGCTGCTGAGGAATGG		TTACGCGTAGTCCGGGACGTCGTACGGGTACATAAGAAATTTTATTTTATGGAGGCG	
TGME49_258360	CACCGCGGTGTTCGTCAGGATCTGCT		TTACGCGTAGTCCGGGACGTCGTACGGGTACCCGTTAAGATGCGCAACGAC	
TGME49_261740	CACCACAAAACGGGGAGCA		TTACGCGTAGTCCGGGACGTCGTACGGGTACGGTCTTTTTCCACCTTTCACACG	
Primers used for gene knock-out (5′–3′)				
TGME49_201860			*GGGGACAAGTTTGTACAAAAAAGCAGGCTTA*TGCTTCGTACGACACCAACG	
			*GGGGACAACTTTGTATAGAAAAGTTG*TGGCTAA	
			TGTATCCACGTGG	
TGME49_201860			*GGGGACAACTTTGTATAATAAAGTTGC*TGAGGTCCAAGCAGCACCGAA	
			*GGGGACCACTTTGTACAAGAAAGCTGGGTA*GAGAGAGTCGGGTTCGTTCG	
TGME49_218270			*GGGGACAAGTTTGTACAAAAAAGCAGGCTTA*AAAGACCTCTCGCCTCGGATT	
			*GGGGACAACTTTGTATAGAAAAGTTGC*TTAGGCTAAGTGTTGGAGC	
TGME49_218270			*GGGGACAACTTTGTATAATAAAGTTGC*TCTAGTCGTCTCGGATGATGG	
			*GGGGACCACTTTGTACAAGAAAGCTGGGTA*TGTCGCTGGAGGATTCATGG	
TGME49_261740			*GGGGACAAGTTTGTACAAAAAAGCAGGCTGCTTA*GTAACCTGCGGATACACTTC	
			*GGGGACAACTTTGTATAGAAAAGTTG*GGGTGGACCGCCGAACATCATTGTTTC	
TGME49_261740			*GGGGACAACTTTGTATAGAAAAGTTG*GGGTGGACCGCCGAACATCATTGTTTC	
			*GGGGACCACTTTCTTGTACAAAGTGGTGGTA*AAGGGCATGTTTTGACACGGG	
	P1	P2	P3	P4
TGME49_201860	CGTGACTTGAAATGCAGTCC	GATCCAGACGTCTTCAATGC	CACCTCGCGACCACCTGCGTTTTGA	TTACGCGTAGTCCGGGACGTCGTACGG GTAGAGTTCAGCGAAAGCACCTGC
TGME49_218270	CACTTCGACTGACATCTCAG	GATCCAGACGTCTTCAATGC	CACCGGCTGGAGATTTTTCCCCGGAACT	TTACGCGTAGTCCGGGACGTCGTACGG GTAAGCCGGACTTGCAGAAGGCAC
Primers used for generation of recombinant ROP47 peptide antigen (5′–3′)				
TGME49_261740	CACCATTTGTCTCGCCGC		CTTTCTTTTTCGACCTTTCACACG	

antibody. For co-localisation experiments, GFP-expressing parasites were fixed with methanol or 3% (vol/vol) formaldehyde. For moving junction staining, this standard IF protocol was modified slightly. Parasites were added to HFFs on coverslips, spun down to bring them into contact with host cells, and allowed to attach to and invade host cells for 5 min at 37 °C. Unattached parasites were washed off with PBS, and cells were fixed with 3% (vol/vol) formaldehyde in PBS for 20 min at room temperature, blocked in PBS with 5% (vol/vol) FBS and 5% (vol/vol) normal goat serum for 1–2 h at room temperature, and permeabilized by incubation in PBS with 0.2% (wt/vol) saponin at 37 °C for 20 min.

2.5. Antibodies

Recombinant ROP47 peptide antigen was generated by PCR amplification of sequences immediately downstream of the predicted ROP47 signal peptide and immediately upstream of the ROP47 stop codon from Pru*Δhxgprt* genomic DNA. The amplicon was cloned in frame into pET102/D-TOPO (Invitrogen), creating a Thioredoxin-ROP47-V5-His6 construct. This protein was expressed in BL21 Star (Invitrogen) cells and purified on a Ni–NTA column (Invitrogen) eluted with 250 mM imidazole and dialyzed under native conditions according to the manufacturer's directions. Rabbit polyclonal antibodies (Covance, USA) were raised against the purified peptide antigen. Antibodies were affinity purified from the ROP47 antiserum with Affi-Gel 10 resin (Bio-Rad) covalently coupled to the antigen peptide and eluted with 100 mM Glycine, pH 2.5, then immediately neutralized with 1 M Tris pH 8.0. The eluate was subsequently incubated with Affi-Gel 10 resin covalently coupled to a Thioredoxin-V5-His6 peptide that was expressed and purified as above to remove antibodies in the serum reacting against thioredoxin and the epitope tags. The flow-through was collected, tested for specificity and used for immunogenic assays.

Antibodies against HA (Roche), *Toxoplasma* surface antigen (SAG)-1 (DG52, (Burg et al., 1988)), *Toxoplasma* rhoptry protein ROP1 (Tg49; (Ossorio et al., 1992)), *Toxoplasma* dense granule protein GRA7 (Dunn et al., 2008), *Toxoplasma* rhoptry neck protein RON4 (generously provided by P. Bradley, University of California, Los Angeles, CA, USA), *Toxoplasma* inner membrane complex proteins IMC1 and MLP1 (generously provided by M.J. Gubbels, Boston College, Boston, MA, USA) and mouse TGTP (A-20; Santa Cruz Biotechnology, USA) were used in the IF assay. IF secondary antibodies were coupled with Alexa Fluor 488 or Alexa Fluor 594 (Invitrogen).

2.6. Western blot

Parasites were syringe lysed from infected HFFs with lysis buffer, boiled for 5 min and subjected to 10% SDS–PAGE. Proteins were transferred to a polyvinylidene difluoride membrane, which was blocked in PBS/0.1% Tween-20/5% non-fat dry milk and incubated with primary and secondary antibodies. The blot was incubated with a luminal-based substrate (Immun-Star WesternC; Bio-Rad Laboratories) and chemiluminescence was detected using a charge-coupled device camera (Chemidoc XRS; Bio-Rad Laboratories). The bands were visualised using Quantity One 1-D analysis software.

2.7. Generation of gene knockouts (KOs)

The 5′ and 3′ flanking regions of the genes to be knocked out were cloned in pTKO2 (Rosowski et al., 2011) around the hypoxanthine–xanthine–guanine ribosyl transferase (HXGPRT) selectable marker using Multisite Gateway Pro 3-Fragment Recombination (Invitrogen). Flanking regions (5′ and 3′) of TGME49_201860, TGME49_218270 and TGME49_261740 were cloned from type II genomic DNA. Primers contained *att* recombination sites (denoted in primer sequence with italics, Table 1) and amplified ≈2 kb upstream of the start codon and downstream of the stop codon. These flanking regions were then cloned around the HXGPRT selectable marker flanked by 5′ and 3′ untranslated region (UTRs) from dihydrofolate reductase (DHFR), as previously described (Rosowski et al., 2011). Before transfection, the KO vector was linearised. Pru*Δhxgprt Δku80* (a gift from D. Bzik, Dartmouth Medical School, Lebanon, NH, USA) parasites were transfected with the KO construct by electroporation, and stable integrants were selected and cloned by limiting dilution, as described in Section 2.3. PCR with a forward primer upstream of the 5′ flanking region (P1) and a reverse primer within the HXGPRT cassette (P2) confirmed the disruption in the desired loci (Supplementary Fig. S1A). Additionally, PCR was performed to confirm the inability to amplify the target genes (P3 and P4) (Supplementary Fig. S1A).

2.8. Plaque assays

For the plaque assays, 100–500 parasites per well were added to monolayers of MEFs seeded the day before and either previously stimulated with 1000 U/mL of mouse IFNγ or left unstimulated for 24 h before infection in a 24 well plate in MEF media. Infections were then incubated for 5 days at 37 °C and the number of plaques was counted using a microscope.

2.9. Animal infections

Six to 10 week old female C57BL/6 J mice (The Jackson Laboratory, USA) were used in all experiments. For i.p. infection, tachyzoites were grown in vitro and extracted from host cells by passage through a 30-gauge needle, washed twice in PBS and quantified with a hemocytometer. Parasites were diluted in PBS and mice were inoculated i.p. with 500 tachyzoites of each strain (in 100 μL) using a 28-gauge needle. For oral infection, brain homogenate of chronically infected mice was stained with dolichos biflorus-FITC (Vector Laboratories) and cysts were enumerated by microscopy. The mice were orally gavaged with 1000 cysts. All of the animals were monitored daily and weighed three times per week. Peripheral blood serum was collected on days 7 and 30 of the experiment and the levels of IFNγ were determined using commercially available ELISA kits, according to the manufacturer's protocol (eBioscience, USA). The Massachusetts Institute for Technology, USA, Committee on Animal Care approved all protocols. All mice were maintained under specific pathogen-free conditions, in accordance with institutional and federal regulations.

3. Results and discussion

3.1. Identification of novel rhoptry proteins

Previous characterisation of the *Toxoplasma* cell cycle transcriptome showed that the mRNA levels of rhoptry encoding genes display the same cyclical expression profile (Behnke et al., 2010). We hypothesised that unidentified rhoptry encoding genes would show a similar expression profile. Genes were identified that showed the same expression pattern as established rhoptry encoding genes by performing K-means clustering of 13 duplicate samples spanning 12 h post-thymidine release into the tachyzoite cell cycle. The cluster with the largest number of previously annotated rhoptry protein encoding genes (67 out of 75 annotated rhoptry encoding genes were expressed above background and were present on the *Toxoplasma* array; Supplementary Table S1) was chosen for further analysis (Table 2, Supplementary Fig. S2). This cluster contained 190 unique genes, of which 45 encoded

Table 2
Toxoplasma genes in the rhoptry cluster. (See below-mentioned references for further information.)

Probeset_id	ToxoDB V8_ID	Product description	Subcellular localisation	Reference	Confirmed	Exons	Transmembrane domains	Predicted signal peptide	Cell cycle microarray RMA	
									Max	Min
20.m08222	TGME49_203990	Rhoptry protein ROP12 (ROP12)	RHOPTRY	Bradley et al. (2005)	Confirmed	3	1	Yes	12.0	7.7
20.m03896	TGME49_205250	Rhoptry protein ROP18 (ROP18)	RHOPTRY	Taylor et al. (2006)	Confirmed	1	1	Yes	13.8	10.6
27.m00091	TGME49_211290	Rhoptry protein ROP15 (ROP15)	RHOPTRY	Bradley et al. (2005)	Confirmed	6	0	Yes	12.7	8.9
33.m02185	TGME49_214080	Toxofilin	RHOPTRY	Bradley et al. (2005)	Confirmed	1	1	Yes	12.2	8.9
33.m01398	TGME49_215775	Rhoptry protein ROP8 (ROP8)	RHOPTRY	Beckers et al. (1997)	Confirmed	1	1	Yes	13.0	9.4
42.m00026	TGME49_223920	Rhoptry neck protein RON3 (RON3)	RHOPTRY	Bradley et al. (2005)	Confirmed	21	1	Yes	12.3	7.9
42.m03584	TGME49_227810	Rhoptry kinase family protein ROP11 (incomplete catalytic triad) (ROP11)	RHOPTRY	Bradley et al. (2005)	Confirmed	1	0	Yes	13.1	9.0
44.m06355	TGME49_229010	Rhoptry neck protein RON4 (RON4)	RHOPTRY	Bradley et al. (2005)	Confirmed	20	0	Yes	11.8	7.7
44.m00026	TGME49_230350	Rhoptry neck protein RON11 (RON11)	RHOPTRY	Beck et al. (2013)	Confirmed	16	4		10.4	6.5
49.m03277	TGME49_242240	Rhoptry kinase family protein ROP19A (ROP19A)	RHOPTRY	Peixoto et al. (2010)	Confirmed	1	0	Yes	10.7	7.4
52.m01543	TGME49_252360	Rhoptry kinase family protein ROP24 (incomplete catalytic triad) (ROP24)	RHOPTRY	Peixoto et al. (2010)	Confirmed	1	0	Yes	11.8	8.0
55.m04748	TGME49_258230	Rhoptry kinase family protein ROP20 (ROP20)	RHOPTRY	Peixoto et al. (2010)	Confirmed	1	1	Yes	10.1	6.5
55.m08191	TGME49_258580	Rhoptry protein ROP17 (ROP17)	RHOPTRY	Peixoto et al. (2010)	Confirmed	1	0	Yes	13.1	9.8
55.m00092	TGME49_258660	Rhoptry protein ROP6 (ROP6)	RHOPTRY	Sohn and Nam (1999)	Confirmed	5	1	Yes	13.3	9.5
55.m00167	TGME49_261750	Rhoptry neck protein RON10 (RON10)	RHOPTRY	Lamarque et al. (2012)	Confirmed	7	0		11.3	6.7
55.m08219	TGME49_262730	Rhoptry protein ROP16 (ROP16)	RHOPTRY	Bradley et al. (2005)	Confirmed	1	0	Yes	11.9	8.5
59.m03479	TGME49_269885	Rhoptry metalloprotease toxolysin TLN1 (TLN1)	RHOPTRY	Hajagos et al. (2011)	Confirmed	12	1	Yes	11.6	6.9
74.m00767	TGME49_282055	Protein phosphatase PP2C-hn (PP2CHN)	RHOPTRY	Gilbert et al. (2007)	Confirmed	13	0		11.5	6.9
80.m02343	TGME49_291960	Rhoptry kinase family protein ROP40 (incomplete catalytic triad) (ROP40)	RHOPTRY	Peixoto et al. (2010)	Confirmed	3	0	Yes	13.1	9.2
83.m02145	TGME49_295110	Rhoptry protein ROP7 (ROP7)	RHOPTRY	Hajj et al. (2006a,b)	Confirmed	1	1	Yes	12.7	8.6
113.m00009	TGME49_297960	Rhoptry neck protein RON6 (RON6)	RHOPTRY	Proellocks et al. (2009)	Confirmed	10	1	Yes	11.5	7.0
129.m00252	TGME49_299060	Sodium/hydrogen exchanger NHE2	RHOPTRY	Karasov et al. (2005)	Confirmed	12	13		10.4	6.5
145.m00331	TGME49_300100	Rhoptry neck protein RON2 (RON2)	RHOPTRY	Bradley et al. (2005)	Confirmed	10	3	Yes	11.4	6.5
541.m00141	TGME49_306060	Rhoptry neck protein RON8 (RON8)	RHOPTRY	Straub et al. (2009)	Confirmed	15	1	Yes	11.9	7.0
551.m00238	TGME49_308090	Rhoptry protein ROP5 (ROP5)	RHOPTRY	Bradley et al. (2005)	Confirmed	1	0	Yes	13.5	10.2
583.m09207	TGME49_308810	Rhoptry neck protein RON9 (RON9)	RHOPTRY	Lamarque et al. (2012)	Confirmed	9	1		10.8	6.5
583.m00003	TGME49_309590	Rhoptry protein ROP1 (ROP1)	RHOPTRY	Ossorio et al. (1992)	Confirmed	1	0	Yes	12.6	9.4
583.m00597	TGME49_310010	Rhoptry neck protein RON1 (RON1)	RHOPTRY	Bradley et al. (2005)	Confirmed	5	1	Yes	11.3	6.8
583.m00636	TGME49_311470	Rhoptry neck protein RON5 (RON5)	RHOPTRY	Straub et al. (2009)	Confirmed	38	0	Yes	12.3	7.6
583.m00692	TGME49_315220	Rhoptry protein ROP14 (ROP14)	RHOPTRY	Bradley et al. (2005)	Confirmed	11	11		10.9	6.5
583.m05686	TGME49_315490	Rhoptry protein ROP10 (ROP10)	RHOPTRY	Bradley et al. (2005)	Confirmed	1	0	Yes	11.1	6.6
49.m05689	TGME49_242118	Myosin-light-chain kinase	RHOPTRY	Peixoto et al. (2010)		1	1		10.8	6.5
20.m00331	TGME49_202200	Hypothetical protein	RHOPTRY	Bradley et al. (2005)		7	0		12.0	7.9
27.m00846	TGME49_211260	Rhoptry kinase family protein ROP26 (incomplete catalytic triad) (ROP26)	RHOPTRY	Peixoto et al. (2010)		2	0		12.7	9.8
41.m01337	TGME49_222100	Hypothetical protein	RHOPTRY	Bradley et al. (2005)		1	0	Yes	11.0	6.5
49.m03276	TGME49_242230	Rhoptry kinase family protein ROP29 (ROP29)	RHOPTRY	Peixoto et al. (2010)		1	1		10.8	6.9
49.m03399	TGME49_244250	Hypothetical protein	RHOPTRY	Bradley et al. (2005)		4	0		11.2	6.9
52.m01529	TGME49_252200	*Toxoplasma* palmitoyl acyltransferase TgDHHC7	RHOPTRY	Beck et al. (2013)		8	4		10.1	6.5
52.m01582	TGME49_253370	Hypothetical protein (RON4L1)	RHOPTRY	Boothroyd and Dubremetz (2008)		30	0	Yes	10.0	6.5
55.m04788	TGME49_258800	Rhoptry kinase family protein ROP31 (ROP31)	RHOPTRY	Peixoto et al. (2010)		1	1	Yes	10.0	6.9
55.m05020	TGME49_262920	Trypsin domain-containing protein	RHOPTRY	Bradley et al. (2005)		11	1	Yes	9.8	6.5
83.m01271	TGME49_294560	Rhoptry kinase family protein ROP37 (incomplete catalytic triad) (ROP37)	RHOPTRY	Peixoto et al. (2010)		1	0	Yes	10.6	6.5
83.m01285	TGME49_294790	Hypothetical protein	RHOPTRY	Bradley et al. (2005)		1	0		13.0	9.7
113.m00755	TGME49_297070	Hypothetical protein	RHOPTRY	Bradley et al. (2005)		2	0	Yes	12.6	8.2
583.m00694	TGME49_315210	Rhoptry protein, putative (ROP14B)	RHOPTRY	Reid et al. (2012)		11	7		10.7	6.5

Table 2 (*continued*)

Probeset_id	ToxoDB V8_ID	Product description	Subcellular localisation	Reference	Confirmed	Exons	Transmembrane domains	Predicted signal peptide	Cell cycle microarray RMA	
									Max	Min
20.m00355	TGME49_201520	Protein phosphatase 2C domain-containing protein				9	0	Yes	11.0	6.6
20.m05880	TGME49_201520	Protein phosphatase 2C domain-containing protein				9	0	Yes	11.0	6.5
20.m03673	TGME49_201760	Hypothetical protein				4	0		10.5	6.5
20.m03682	TGME49_201860	Hypothetical protein				2	1	Yes	13.3	9.8
20.m03718	TGME49_202420	Hypothetical protein				2	1		9.2	6.5
20.m00003	TGME49_202500	GAPM1a				4	6		13.7	10.2
20.m03760	TGME49_203010	Aurora kinase				1	0		9.9	6.5
20.m05981	TGME49_203930	Hypothetical protein				6	5		10.6	6.6
20.m03880	TGME49_204880	Hypothetical protein				1	0	Yes	9.3	6.5
20.m03902	TGME49_205330	Hypothetical protein				2	8		12.7	8.6
20.m03905	TGME49_205360	Hypothetical protein				20	2	Yes	9.7	6.5
20.m03977	TGME49_206710	Hypothetical protein				5	0		8.5	6.5
25.m01833	TGME49_208910	Hypothetical protein				3	0		9.2	6.5
25.m01852	TGME49_209170	Hypothetical protein				1	0	Yes	9.6	6.5
25.m01855	TGME49_209200	Hypothetical protein				12	0		9.0	6.5
25.m01859	TGME49_209250	Hypothetical protein				7	1		10.8	7.8
26.m00235	TGME49_210270	Hypothetical protein				3	0		10.1	7.6
26.m00242	TGME49_210370	Hypothetical protein				1	0	Yes	12.2	8.2
26.m00370	TGME49_210420	Hypothetical protein				1	1		11.3	7.1
27.m00828	TGME49_210820	Hypothetical protein				3	10		9.3	6.5
28.m00429	TGME49_211850	Hypothetical protein				3	0		11.8	9.1
31.m00934	TGME49_212980	Hypothetical protein				2	1		11.8	8.6
33.m02670	TGME49_214400	Hypothetical protein				2	0		10.7	6.7
35.m00004	TGME49_216080	Apical complex lysine methyltransferase				4	0		11.3	8.3
35.m00895	TGME49_216620	EF hand domain-containing protein				39	7		9.0	6.5
37.m00748	TGME49_217520	Hypothetical protein				2	0	Yes	12.5	8.8
38.m01037	TGME49_218240	Hypothetical protein				2	1	Yes	9.6	6.5
38.m01040	TGME49_218270	Hypothetical protein				1	8	Yes	12.7	8.4
41.m01283	TGME49_221250	Hypothetical protein				8	0		9.8	6.5
41.m00036	TGME49_221620	Beta-tubulin, putative				4	0		13.1	9.7
41.m01316	TGME49_221675	Hypothetical protein				9	1	Yes	8.9	6.5
42.m03399	TGME49_225020	Hypothetical protein				4	0		9.5	6.5
42.m03409	TGME49_225160	Hypothetical protein				1	2	Yes	11.5	7.8
42.m07438	TGME49_225200	Hypothetical protein				33	0	Yes	9.2	6.5
42.m00061	TGME49_225320	Hypothetical protein				5	0	Yes	10.8	6.5
42.m00060	TGME49_225330	Hypothetical protein				6	0	Yes	9.8	6.5
42.m03456	TGME49_225860	Hypothetical protein				4	0		9.8	6.5
42.m03481	TGME49_226220	Alveolin domain containing intermediate filament IMC9 (ALV6/IMC9)				9	0		9.7	6.5
42.m00093	TGME49_227000	Hypothetical protein				16	0		9.9	6.5
44.m02549	TGME49_229500	Hypothetical protein				2	3		9.8	6.6
44.m02600	TGME49_230480	Hypothetical protein				1	2		11.4	7.5
44.m02630	TGME49_231000	START domain-containing protein				18	1		9.0	6.5
44.m02636	TGME49_231070	Protein kinase				1	0		10.8	6.8
44.m02644	TGME49_231160	Hypothetical protein				3	0		12.7	9.5
44.m02678	TGME49_231840	Hypothetical protein				6	0		9.7	6.5
44.m02696	TGME49_232020	Hypothetical protein				2	1		8.8	6.5
44.m02714	TGME49_232260	Hypothetical protein				3	3		10.0	6.5
44.m02750	TGME49_232780	Hypothetical protein				8	0		9.5	6.5
46.m01616	TGME49_234540	Hypothetical protein				7	9		10.2	6.5
46.m02875	TGME49_235130	Transmembrane protein				4	0	Yes	9.3	6.5
46.m01643	TGME49_235380	Hypothetical protein				11	0		8.9	6.5

46.m01716	TGME49_236860	Haloacid dehalogenase family hydrolase domain-containing protein	2	12		9.8	6.5
46.m01722	TGME49_236960	Transporter, major facilitator family protein	10	10		10.8	6.8
46.m01740	TGME49_237180	Hypothetical protein	1	0	Yes	12.1	7.8
46.m01741	TGME49_237190	Hypothetical protein	4	0		9.7	6.5
46.m01743	TGME49_237210	Tyrosine kinase-like (TKL) protein	4	0		10.2	6.5
49.m03087	TGME49_238150	Hypothetical protein	1	8		12.7	10.2
49.m03179	TGME49_239830	TBC domain-containing protein	13	0		10.7	6.5
49.m03213	TGME49_240460	AP2 domain transcription factor AP2VI-1 (AP2VI1)	2	0		10.9	6.8
49.m07198	TGME49_240730	Hypothetical protein	2	4		9.0	6.5
49.m07245	TGME49_241000	Hypothetical protein	1	4		11.0	7.0
49.m03332	TGME49_243200	Hypothetical protein	5	0		12.2	6.6
49.m00056	TGME49_243690	Hypothetical protein	4	1		12.1	8.0
49.m03388	TGME49_244080	Hypothetical protein	3	1	Yes	10.7	6.5
49.m03412	TGME49_244470	Hypothetical protein	8	0		10.0	7.0
50.m03074	TGME49_245550	Hypothetical protein	1	4	Yes	10.0	6.5
50.m03107	TGME49_246182	Hypothetical protein				10.1	7.2
50.m03131	TGME49_246710	Hypothetical protein	1	3		9.0	6.5
50.m03132	TGME49_246720	Hypothetical protein	1	0		10.2	7.2
50.m03154	TGME49_247195	Microneme protein MIC15 (MIC15)	42	1	Yes	9.8	6.5
50.m03253	TGME49_248690	Hypothetical protein	7	0		9.4	6.8
50.m03302	TGME49_249440	Hypothetical protein	2	0		9.9	6.5
50.m03315	TGME49_249570	Hypothetical protein	20	1	Yes	11.4	6.8
52.m01567	TGME49_253140	Hypothetical protein	3	0		9.3	6.5
52.m01583	TGME49_253380	AP2 domain transcription factor AP2III-2 (AP2III2)	1	0		10.5	6.8
52.m01598	TGME49_253600	Hypothetical protein	11	0		9.6	6.5
52.m01644	TGME49_254290	Hypothetical protein	1	0		9.0	6.5
55.m04629	TGME49_255700	Hypothetical protein	6	0		9.7	6.5
55.m08188	TGME49_256030	Hypothetical protein	6	0		12.1	7.6
55.m04752	TGME49_258360	Hypothetical protein	7	0	Yes	11.6	7.0
55.m00096	TGME49_258700	Transporter, major facilitator family protein	12	11		9.3	6.5
55.m04796	TGME49_258900	Hypothetical protein	4	0		9.3	6.5
55.m04843	TGME49_259700	Hypothetical protein	2	3		11.1	6.9
55.m00144	TGME49_260820	IMC sub-compartment protein ISP1 (ISP1)	3	0		12.0	8.5
55.m04955	TGME49_261740	Hypothetical protein	1	1	Yes	14.2	11.9
57.m01689	TGME49_264600	Hypothetical protein	2	4		12.2	7.5
57.m01720	TGME49_265080	Tubulin-tyrosine ligase family protein	12	0		9.6	6.5
57.m01755	TGME49_265650	Protein phosphatase 2C domain-containing protein	1	0	Yes	9.7	6.5
57.m01783	TGME49_266300	Hypothetical protein	2	0		12.3	8.0
57.m01792	TGME49_266435	Hypothetical protein	34	0		9.4	6.5
57.m01834	TGME49_267070	Aquaporin 2	1	11		11.6	7.7
59.m03403	TGME49_268760	Hypothetical protein				12.2	8.6
59.m00087	TGME49_268870	Tetratricopeptide repeat-containing protein	10	0		10.3	6.5
59.m00092	TGME49_269330	Hypothetical protein	10	0		10.1	6.6
59.m00029	TGME49_269340	Hypothetical protein	4	1		11.4	6.9
59.m03542	TGME49_270890	Hypothetical protein	3	0		9.4	6.5
59.m00038	TGME49_271270	Hypothetical protein	10	1		11.2	7.0
59.m03707	TGME49_273860	Hypothetical protein	1	0		11.0	8.2
64.m00327	TGME49_275670	Alveolin domain containing intermediate filament IMC15 (ALV5/IMC15)	9	0		10.8	6.5
64.m00582	TGME49_276130	Cathepsin CPC2 (CPC2)	10	0	Yes	9.7	6.5
65.m01152	TGME49_278130	Hypothetical protein	14	0		9.3	6.5
65.m01964	TGME49_278510	Protein phosphatase 2C domain-containing protein	10	1	Yes	11.1	7.3
65.m02537	TGME49_278920	Hypothetical protein	5	6		9.5	6.5
69.m00143	TGME49_279420	Hypothetical protein	1	0		11.3	6.5
72.m00385	TGME49_280480	EF hand domain-containing protein	1	4		11.5	6.8
72.m00685	TGME49_280670	Hypothetical protein	7	10	Yes	11.3	6.7
74.m00455	TGME49_282070	Hypothetical protein	9	0		10.8	6.5
74.m00465	TGME49_282210	AP2 domain transcription factor AP2VIIa-8 (AP2VIIA8)	2	0		9.3	6.5

Table 2 (*continued*)

Probeset_id	ToxoDB V8_ID	Product description	Subcellular localisation	Reference	Confirmed	Exons	Transmembrane domains	Predicted signal peptide	Cell cycle microarray RMA	
									Max	Min
76.m01597	TGME49_285290	Hypothetical protein				1	3	Yes	10.3	6.5
76.m01608	TGME49_285650	Hypothetical protein				2	0		8.9	6.5
76.m01626	TGME49_285870	SAG-related sequence SRS20A (SRS20A)				2	1	Yes	12.8	8.7
76.m01662	TGME49_286500	Hypothetical protein				1	10		9.9	6.5
80.m02122	TGME49_287970	Hypothetical protein				3	0		10.4	6.5
80.m02181	TGME49_288950	AP2 domain transcription factor AP2IX-4 (AP2IX4)				1	0		9.7	6.5
80.m03982	TGME49_289150	Hypothetical protein				5	1		9.4	6.5
80.m03946	TGME49_289970	Hypothetical protein				3	0		11.7	9.3
83.m01220	TGME49_293540	Hypothetical protein				6	0		10.3	6.5
83.m01311	TGME49_295100	Hypothetical protein				4	0		9.5	6.9
86.m00370	TGME49_295420	Hypothetical protein				9	0		10.4	7.0
86.m00377	TGME49_295620	Hypothetical protein				4	0		9.7	6.5
113.m01286	TGME49_298010	Hypothetical protein				52	0		9.1	6.5
145.m00603	TGME49_300220	Hypothetical protein				15	4	Yes	9.4	6.5
145.m00607	TGME49_300360	ADP/ATP translocase				6	2		9.5	6.5
162.m00326	TGME49_301420	Hypothetical protein				7	0		11.8	7.5
541.m00127	TGME49_305250	Hypothetical protein				6	6		10.5	7.1
541.m01166	TGME49_305270	Hypothetical protein				6	0	Yes	10.2	6.5
541.m00131	TGME49_305510	Hypothetical protein				7	0	Yes	11.9	7.9
541.m01185	TGME49_305590	ABC transporter transmembrane region domain-containing protein				9	9		9.5	6.5
542.m00226	TGME49_307020	Hypothetical protein				3	0		9.4	6.5
551.m00232	TGME49_308010	Hypothetical protein				1	0		9.0	6.5
583.m05275	TGME49_309160	IgA-specific metalloendopeptidase				1	0	Yes	10.4	6.5
583.m09102	TGME49_310240	Hypothetical protein				1	2		10.3	6.5
583.m11449	TGME49_310740	Hypothetical protein				2	7		9.3	6.5
583.m00659	TGME49_311800	Endonuclease/exonuclease/phosphatase family protein				6	0		9.1	6.6
583.m00645	TGME49_312150	Hypothetical protein				6	1		11.7	7.6
583.m09217	TGME49_313780	Hypothetical protein				1	0		11.1	7.3
583.m09134	TGME49_314260	Hypothetical protein				1	1		12.1	8.2
583.m05709	TGME49_315780	Myosin regulatory light chain, putative				7	0		11.5	8.6
583.m05738	TGME49_316260	Hypothetical protein				2	7		12.3	8.1
583.m09158	TGME49_316280	Transporter, major facilitator family protein				4	8		11.7	7.3
583.m05758	TGME49_316540	IMC sub-compartment protein ISP3 (ISP3)				1	0		11.1	8.0
611.m00052	TGME49_317705	Enoyl-CoA hydratase/isomerase family protein				8	0		10.5	7.2
641.m01483	TGME49_318470	AP2 domain transcription factor AP2IV-4 (AP2IV4)				1	0		9.3	6.5
641.m00181	TGME49_320740	Hypothetical protein				5	1	Yes	11.7	8.6
645.m00324	TGME49_321600	Hypothetical protein				7	0		9.6	6.5

Genes highlighted in grey were further characterised in this study.

RMA, Robust Multi-array Average.

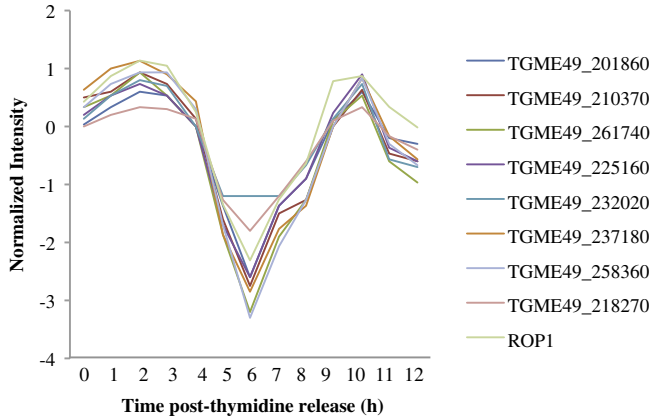

Fig. 1. Identification of new *Toxoplasma* rhoptry proteins. The gene expression profile of the entire genome of *Toxoplasma* was compared with the cyclical gene expression profile of rhoptry genes throughout the cell cycle by performing clustering of duplicate samples spanning 12 h post-synchronisation (Supplementary Fig. S2). Shown are eight genes that displayed an expression profile signature similar to the rhoptry pattern and that were chosen for further analysis. The expression profile of ROP1 is also shown.

proteins annotated as rhoptries (out of 67 possible genes) and four encoded IMC proteins. Thirty-one out of these 45 have been previously confirmed to localise to the rhoptry organelles.

The *Toxoplasma* genome is predicted to encode 8127 genes, 1920 of which have a signal peptide (23.4%). Our analysis imposed no explicit selection for genes coding for proteins with signal peptide sequences; however, the resulting list is enriched (65 genes with a predicted signal peptide out of 190, $P = 0.0003$, Hypergeometric distribution) in signal-peptide-containing proteins (34%).

Interestingly, 22 out of the 75 tachyzoite rhoptry proteins encoding genes never clustered with the remainder of the rhoptries (Supplementary Table S1). Two of these genes (RON2L1 and BRP1 (Schwarz et al., 2005; Fritz et al., 2012)) encode bradyzoite- or sporozoite-specific rhoptry proteins and six encode confirmed tachyzoite rhoptries (ROP9, ROP38, ROP39, TgARO, Toxolysin 1 and Subtilisin 2). According to the cell cycle expression data (Behnke et al., 2010), ROP9, ROP38 and ROP39 do not display an obvious cyclical expression profile. In addition, ROP9 was shown to be secreted with micronemal proteins, in a calcium-dependent manner (Kawase et al., 2007). The cellular localisation of the proteins encoded by the other 14 genes annotated as rhoptry protein genes (Supplementary Table S1) was never confirmed by IF and it is therefore possible that these are not localised to the rhoptries.

These results underscore the relevance of our approach and strongly suggest that our rhoptry protein cluster might contain many of the remainder of the unidentified rhoptry protein-encoding genes of tachyzoites. To identify new putative rhoptry protein encoding genes that could modulate host cell functions, we chose eight genes that encoded a protein with a predicted signal peptide, unannotated function and unknown subcellular localisation from

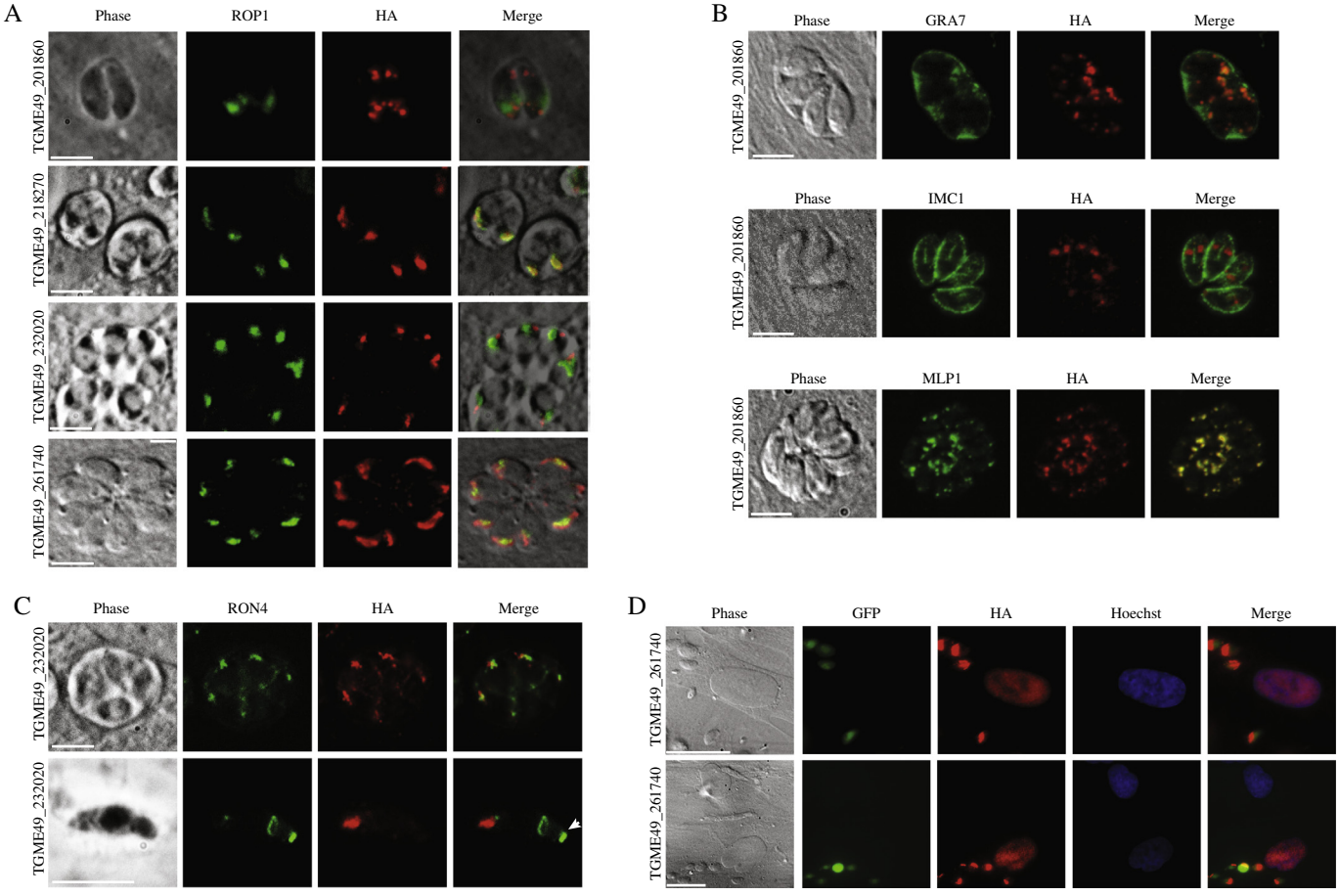

Fig. 2. Cellular localisation of C-terminally tagged genes. Human foreskin fibroblasts (HFFs) were infected with RH expressing hemagglutinin (HA)-tagged TGME49_201860, TGME49_218270 (*rop48*), TGME49_232020 (*ron12*) or TGME49_261740 (*rop47*), fixed and stained with (A) α-HA and rhoptry protein marker α-ROP1, (B) α-HA and dense granule protein marker α-GRA7, α-HA and inner membrane complex marker α-IMC1, α-HA and inner membrane complex marker α-MLP1. (C) α-HA and rhoptry neck/moving junction marker, α-RON4 and (D) α-HA, α-ROP47 and Hoechst dye. (A–C) Scale bars represent 5 μm. (D) Scale bars represent 20 μm.

Table 3
Characteristics of new putative rhoptry protein encoding genes identified in this study.

Candidate gene Alias ToxoDB V8 ID	Signal peptide	Transmembrane domains	Conserved domains	Paralogue (% protein identity)	Paralogue present in rhoptry cluster	Homologue in *Neospora caninum* (% protein identity)
TGME49_201860–	Yes	1	–	TGME49_301390 (31%)	No	NCLIV_022900 (75%)
TGME49_218270ROP48	Yes	8	–	TGME49_209810 (29%)	No	NCLIV_061950 (71%)
TGME49_232020RON12	Yes, in GT1 and CEP	1	–	TGME49_244726 (27%)	No	NCLIV_032020 (59%)
TGME49_261740ROP47	Yes	1	–	–		NCLIV_025740 (43%)

within our rhoptry cluster. The eight candidate genes are described in Table 2, highlighted in grey, and all display the cyclic expression profile described above (Fig. 1).

To determine the localisation of the candidate gene products within the parasite, we genetically engineered *Toxoplasma* strains expressing an HA-tagged version of the candidate genes at their endogenous loci. We were unable to endogenously tag TGME49_261740 and therefore determined its localisation by heterologous expression of a C-terminal HA-tagged copy of the candidate gene, including at least 1500 bp of the putative endogenous promoter. The correct tagging of each endogenously tagged gene was confirmed by PCR (Supplementary Fig. S3). IF analysis was performed on HFFs infected with each of the HA-tagged parasites. The staining pattern of four out of eight candidate gene products was unlike that of the secretory organelles and appeared to label the whole parasite (Supplementary Fig. S4). The genes whose labeling appeared consistent with that of the secretory organelles were TGME49_201860, TGME49_218270, TGME49_232020 and TGME49_261740 (Fig. 2A). Some characteristics of the proteins encoded by these genes are described in Table 3.

The product of TGME49_201860-HA appears to have a punctate distribution, present at both the posterior and the apical end of the parasite (Fig. 2A). TGME49_218270-HA seems to label the rhoptry bulb. We were unable to detect these two proteins using an anti-HA Western blot, and therefore do not know whether they undergo post-transcriptional processing.

TGME49_232020-HA localises to the apical pole of the parasite, a labeling consistent with the rhoptry neck (Fig. 2A). This gene is predicted to encode a protein with no signal peptide in type II parasites. However, as first exon prediction is notoriously difficult, in type I and type III parasites, this protein is predicted have a signal peptide. Moreover, TGME49_232020 encodes a protein with a predicted molecular weight of 135 kDa. However, Western blot analysis of the TGME49_232020-HA strain detected a band of approximately 40 kDa, instead of the predicted 135 kDa (Supplementary Fig. S5). Indeed, several rhoptry proteins exhibit N-terminal processing and that is also probably the case for TGME49_232020. The rhoptry subtilisin TgSUB2 recognises and cleaves after the consensus sequence SΦXE (Miller et al., 2003). There is a putative SUB2 cleavage site (SPQE) between amino acids 968 and 971 of TGME49_232020. Cleavage at this site would generate a ~32 kDa tagged product, which could be consistent with the band observed. Longer exposures did not reveal a 135 kDa pro-protein, suggesting that the half-life of the pro-protein is very short.

TGME49_261740-HA appears to label the entire rhoptry organelle (Fig. 2A). Interestingly, TGME49_261740 is in the top five of the most highly expressed genes across the *Toxoplasma* cell cycle (Behnke et al., 2010) and is one of the most polymorphic *Toxoplasma* genes (Minot et al., 2012). Anti-HA Western blotting of this protein detected a band of approximately 15 kDa, consistent with the predicted size of 14 kDa (Supplementary Fig. S1B).

These four proteins are conserved between *Toxoplasma* and *Neospora* (Table 3), but protein BLAST analysis did not reveal the presence of close (30% or more protein identity) homologues in other apicomplexans. Additionally, no known conserved domains were detected, giving no indication about the potential function of these proteins.

3.2. TGME49_218270, TGME49_232020 and TGME49_261740 encode new rhoptry proteins

To further confirm the localisation of TGME49_201860, TGME49_218270, TGME49_232020 and TGME49_261740 within the parasite, we performed co-staining of each protein with a rhoptry bulb marker, ROP1, on intracellular parasites (Fig. 2A). TGME49_218270-HA shows a perfect co-localisation with ROP1.

TGME49_201860-HA does not overlap with this rhoptry marker. To further investigate the cellular localisation of this protein, we co-stained the TGME49_201860-HA expressing parasites with

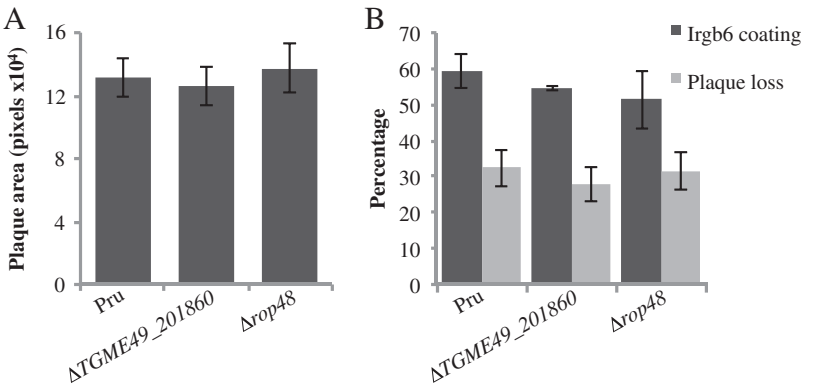

Fig. 3. Deletion of TGME49_201860 and ROP48 does not affect plaque loss in response to IFNγ. (A) Monolayers of mouse embryonic fibroblasts (MEF) were infected with PruΔ*hxgprt*Δ*ku80*, Δ*TGME49_201860* or Δ*rop48* parasites. The plaque area was quantified after 5 days. Mean ± SD; $n \geqslant 30$ plaques. (B) Quantification of the localisation of IFNγ-inducible immunity-related GTPase B6 (Irgb6) on the parasite containing vacuole and of the percentage of plaque loss after 5 days on MEF stimulated with IFNγcompared with unstimulated MEF. Mean ± SD; $n = 4$ experiments.

dense granule (GRA7) and inner membrane complex (IMC1 and MIP1-like protein-1 (MLP1)) markers (Fig. 2B). TGME49_201860-HA appears to partially overlap with GRA7. In addition, while it does not co-localise with IMC1, it co-localises with MLP1, a protein that is present at the apical cap and basal complex of mature as well as budding daughter parasites (Gubbels, personal communication).

TGME49_232020-HA showed labeling of the apical pole anterior to the rhoptry bulb protein ROP1, as well as co-localisation with RON4 staining (Fig. 2C), confirming rhoptry neck localisation in intracellular parasites. Interestingly, TGME49_232020-HA does not localise to the moving junction in invading parasites (Fig. 2C). It was recently shown that RON9, RON10 and RON11, in contrast to the other RONs described to date, do not relocalise from the rhoptry neck to the moving junction during host invasion (Lamarque et al., 2012; Beck et al., 2013). TGME49_232020 localisation also seems to be independent of the moving junction. Similar to TGME49_232020, RON10 has a predicted signal peptide in its N-terminus but no known domains or motifs have been identified. In contrast, RON9 harbors several protein–protein interaction domains. The disruption of either RON9 or RON10 led to the retention of either protein in the endoplasmic reticulum (ER), suggesting an interaction between RON9 and RON10 during their trafficking through the secretory pathway on the way to the rhoptries. Whether TGME49_232020 can interact with the RON9/RON10 complex or any other rhoptry neck protein in a similar fashion remains to be determined. TGME49_261740 co-localises with ROP1 (Fig. 2B) and is also found in the nucleus of infected host cells (Fig. 2D). NLS Mapper (Kosugi et al., 2009) predicts that TGME49_261740 (ROP47) encodes a bipartite NLS with a score of 3.4. Moreover, this protein is predicted to have a size of 15 kDa and is probably able to diffuse through nuclear pores.

Altogether, these results suggest that TGME49_261740 and TGME49_218270 encode new rhoptry bulb proteins, hereafter referred to as ROP47 and ROP48, respectively. TGME49_232020 codes for a new rhoptry neck protein, from now on referred to as RON12.

3.3. TGME49_201860 and ROP48 are not implicated in evasion of the IFNγ response

To investigate the role of TGME49_201860, ROP47 and ROP48 in parasite biology, we removed these genes in the *PruΔhxgprtΔku80* strain using double homologous recombination. PCR confirmed both the absence of the target gene coding sequences and the insertion of the *hxgprt* gene in the parasite genome. The deletion of ROP47 was confirmed by western blot (Supplementary Fig. S1B). Our attempts to generate a KO of RON12 in the *PruΔhxgprtΔku80* strain have to date been unsuccessful.

To determine a potential growth phenotype, monolayers of MEF were infected with PruΔ*hxgprtΔku80*, Δ*tgme49_201860* or Δ*rop48* parasites, the parasites were allowed to grow for 5 days, and then the areas of the plaques formed on the monolayers were quantified

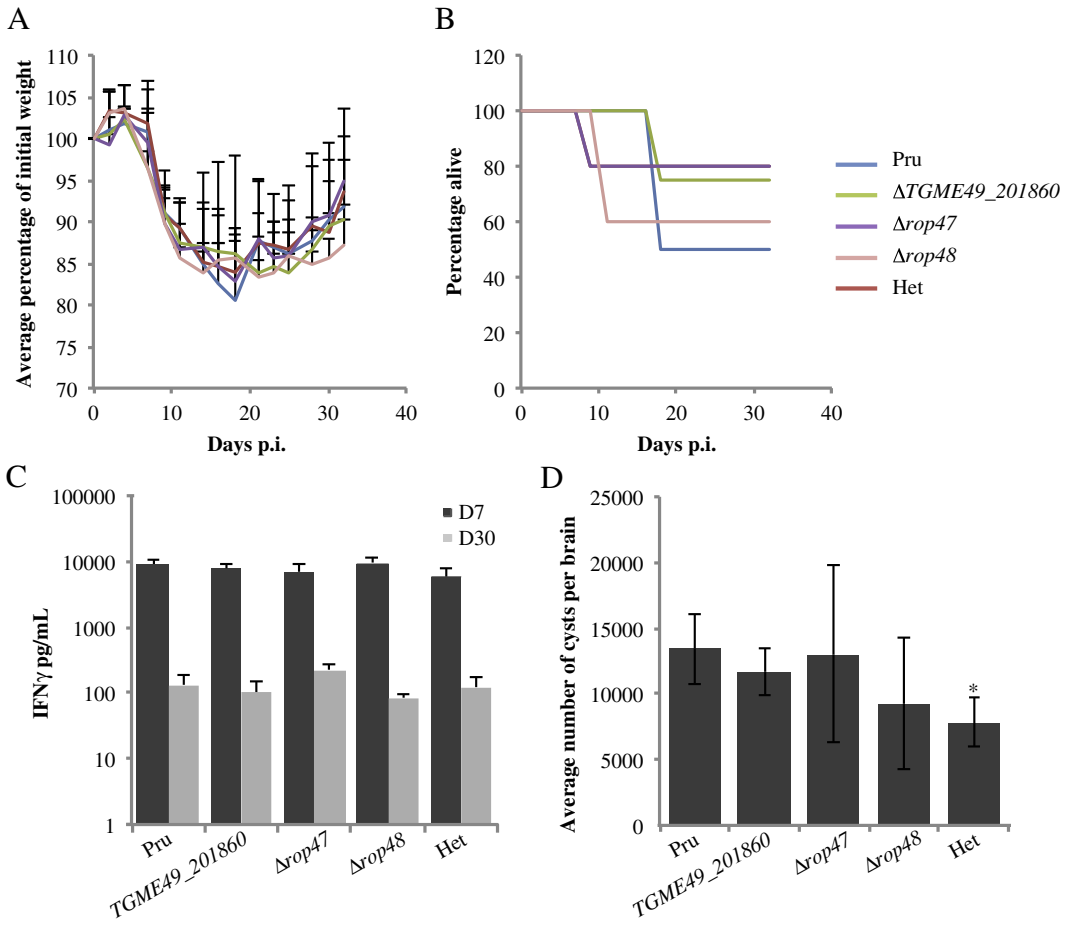

Fig. 4. Deletion of the genes encoding TGME49_201860, ROP47 and ROP48 does not affect *Toxoplasma gondii* virulence in mice. C57BL/6 mice were infected with 500 tachyzoites and weight and survival of mice was monitored. (A) Average percentage change in weight over time for mice i.p. infected with the indicated strains; $n \geqslant 4$ for each strain, mean + SD. (B) Mouse survival after i.p. infection with indicated strains; $n \geqslant 4$ for each strain. (C) IFNγ cytokine levels in peripheral blood serum of surviving animals ($n \geqslant 2$ for each strain) was determined by ELISA at days 7 (D7) and 30 (D30) p.i., mean ± SD. Pru, *PruΔhxgprtΔku80*. Het, Heterologous control. (D) Average number of brain cysts at day 35 following i.p. infection with the indicated strains; $n \geqslant 2$ for each strain; mean ± SD. Pru – *PruΔhxgprtΔku80*. Het – Heterologous control. $^{*}P = 0.0011$, Student's *t*-test.

(Fig. 3A). PruΔ*hxgprtΔku80*, Δ*tgme49_201860* and Δ*rop48* strains did not form significantly different sized plaques. These data indicate that deletion of TGME49_201860 or ROP48 has no major influence on in vitro *Toxoplasma* growth.

It is well established that IFNγ is the main mediator of resistance against *Toxoplasma* (Suzuki et al., 1988). An important class of downstream effectors of this immune activation is the IFNγ-inducible immunity-related GTPases (IRGs), which belong to the dynamin family of GTPases and can cooperatively oligomerize to vesiculate membranes. The IRGs are able to disrupt the PVM and kill the parasite (Butcher et al., 2005). Recently, two rhoptry proteins were shown to mediate *Toxoplasma* evasion of the IFNγ–induced IRGs in murine cells (Fentress et al., 2010; Steinfeldt et al., 2010; Niedelman et al., 2012). To study a potential role of ROP48 and TGME49_201860 in *Toxoplasma* resistance to IFNγ and the IRGs, we measured the percentage of vacuoles coated with Irgb6 by IF in IFNγ-stimulated MEFs infected with PruΔ*hxgprtΔku80*, Δ*tgme49_201860* or Δ*rop48*. The percentage of coated vacuoles was approximately 50% in both Δ*tgme49_201860* and Δ*rop48* and was not significantly different from that of the parental strain, PruΔ*hxgprtΔku80* (Fig. 3B). Although it is generally assumed that once the PVM is coated, it will eventually lead to killing of the parasite inside, it has also been shown that *Toxoplasma* can escape a coated vacuole and invade a new cell (Zhao et al., 2009). Therefore, to measure killing of *Toxoplasma*, a plaque loss assay was performed, as described in Niedelman et al. (2012). Briefly, 100 parasites were seeded on a monolayer of MEF, either previously stimulated for 24 h with IFNγ or left untreated, and the number of plaques that form after 5 days of growth was determined. The three strains had an average of ~30% plaque loss when comparing plaques formed on IFNγ-stimulated MEFs with unstimulated MEFs. This percentage of plaque loss was lower than the percentage of vacuoles coated with Irgb6, suggesting that some coated vacuoles can escape destruction by the IRGs. Overall, the results suggest that TGME49_201860 and ROP48 are not implicated in evading the IFNγ response in MEFs. Indeed, ROP5 and ROP18 were recently reported to mediate *Toxoplasma* evasion of the murine IFNγ response (Niedelman et al., 2012). These two proteins seem to determine the majority of strain differences in mouse IRG evasion, even for non-clonal strains for which virulence determinants have not been studied. However, neither ROP18 nor ROP5 markedly affect survival in IFNγ-activated human cells and it is reasonable to speculate that one or more still unidentified, secreted, potentially a rhoptry, protein could be involved in escaping IFNγ-mediated killing in other host cell types. Whether this (these) protein(s) can be found within the rhoptry cluster will be the object of future studies.

3.4. TGME49_201860, ROP47 and ROP48 are not implicated in *Toxoplasma* virulence in mice

To examine the role of TGME49_201860, ROP47 and ROP48 on parasite virulence, we infected C57BL/6 mice by i.p. injection with 500 tachyzoites of PruΔ*hxgprtΔku80*, Δ*tgme49_201860*, Δ*rop47*, Δ*rop48* or a heterologous control strain (Het) and assessed mouse morbidity (through monitoring of weight loss) and survival during the initial phase of infection (days 0–32) (Fig. 4A, B). Weight loss started at day 4 p.i. The mice reached their lowest weight between days 14 and 18 (~80% of their initial body weight) and did not regain their original weight. The survival of C57BL/6 mice infected with either strain did not show significant differences compared with PruΔ*hxgprtΔku80* infected mice ($P = 0.9060$, Log-rank Mantel-Cox test). Seroconversion was examined at day 30 p.i. and all the animals tested seropositive (data not shown). The level of IFNγ in peripheral blood serum was measured at day 7 and day 30 p.i. (Fig. 4D). IFNγ levels were higher at day 7 than day 30 and similar for all the strains. Prior to infection, animals did not display detectable levels of IFNγ. At day 35 p.i., the surviving mice were sacrificed and the number of brain cysts per mouse was determined (Fig. 4C). The numbers of cysts generated by the Δ*tgme49_201860*, Δ*rop47* and Δ*rop48* parasites were not significantly different from that of their parental strain. The number of brain cysts observed in the mice injected i.p. with the heterologous control strain was significantly lower (~1.6-fold, $P = 0.0011$, Student's *t*-test) than that observed in mice infected with PruΔ*hxgprtΔku80* parasites. Accordingly, it was previously reported that PruΔ*ku80::hxgprt* exhibited lower cyst burdens than PruΔ*hxgprtΔku80* (Fox et al., 2011), which suggests the presence of HXGPRT might affect generation or viability of brain cysts. Additionally, we infected C57BL/6 mice by oral gavage with 1000 brain cysts of the same strains. We found no difference in mouse morbidity and survival (data not shown).

Overall, the results suggest that TGME49_201860, ROP47 and ROP48 are not implicated in *Toxoplasma* virulence in mice. Interestingly, relatively few rhoptry proteins seem to have been investigated on their ability to affect virulence in the mouse model. Of the 10 proteins that were reported, ROP5, ROP16, ROP13, ROP18, RON8, RON9/10, TLN1, BRP1 and PP2C-hn (Saeij et al., 2006; Gilbert et al., 2007; Turetzky et al., 2010; Hajagos et al., 2011; Straub et al., 2011; Lamarque et al., 2012; Niedelman et al., 2012;), only four (RON8, ROP5, ROP16, ROP18) have an effect on mouse survival. However, mouse virulence is often tested in tachyzoites, the asexually reproducing form of the parasite, leaving out events that are restricted to the sexual life cycle of the parasite. Alternatively, the mouse model used may not be the optimal setting to reveal an essential role for such proteins in infection. For instance, a role in virulence could only be apparent in other intermediate hosts and/or when cysts are ingested naturally. Elucidation of this question will be extremely challenging due to the remarkable host range of *Toxoplasma*.

Acknowledgements

The authors thank V. Carruthers for RHΔ*hxgprtΔku80*, D. Bzik for PruΔ*hxgprtΔku80*, P. Bradley for the anti-RON4 antibody, M.J. Gubbels for the anti-IMC1 and anti-MLP1 antibodies, and the members of the Saeij laboratory for helpful discussions. This work was supported by a postdoctoral fellowship from the American Heart Association to A.C., a postdoctoral fellowship from the Knights Templar Eye Foundation, USA, to D.A.G., an A*STAR NSS, Singapore, graduate scholarship to N.Y., postdoctoral fellowships from the Cancer Research Institute, USA, and the Charles A. King Trust, USA, to K.D.C.J. and National Institutes of Health, USA Grant R01-AI080621 to J.P.J.S.

Appendix A. Supplementary data

Supplementary data associated with this article can be found, in the online version, at http://dx.doi.org/10.1016/j.ijpara.2013.08.002.

References

Beck, J.R., Fung, C., Straub, K.W., Coppens, I., Vashisht, A.A., Wohlschlegel, J.A., Bradley, P.J., 2013. A *Toxoplasma* palmitoyl acyl transferase and the palmitoylated armadillo repeat protein TgARO govern apical rhoptry tethering and reveal a critical role for the rhoptries in host cell invasion but not egress. PLoS Pathog. 9, e1003162.

Beckers, C.J., Wakefield, T., Joiner, K.A., 1997. The expression of *Toxoplasma* proteins in *Neospora caninum* and the identification of a gene encoding a novel rhoptry protein. Mol. Biochem. Parasitol. 89, 209–223.

Behnke, M.S., Fentress, S.J., Mashayekhi, M., Li, L.X., Taylor, G.A., Sibley, L.D., 2012. The polymorphic pseudokinase ROP5 controls virulence in *Toxoplasma gondii* by regulating the active kinase ROP18. PLoS Pathog. 8, e1002992.

Behnke, M.S., Wootton, J.C., Lehmann, M.M., Radke, J.B., Lucas, O., Nawas, J., Sibley, L.D., White, M.W., 2010. Coordinated progression through two subtranscriptomes underlies the tachyzoite cycle of *Toxoplasma gondii*. PLoS ONE 5, e12354.

Besteiro, S., Michelin, A., Poncet, J., Dubremetz, J.-F., Lebrun, M., 2009. Export of a *Toxoplasma gondii* rhoptry neck protein complex at the host cell membrane to form the moving junction during invasion. PLoS Pathog. 5, e1000309.

Boothroyd, J.C., Dubremetz, J.-F., 2008. Kiss and spit: the dual roles of *Toxoplasma* rhoptries. Nat. Rev. Microbiol. 6, 79–88.

Bradley, P.J., Boothroyd, J.C., 1999. Identification of the pro-mature processing site of *Toxoplasma* ROP1 by mass spectrometry. Mol. Biochem. Parasitol. 100, 103–109.

Bradley, P.J., Hsieh, C.L., Boothroyd, J.C., 2002. Unprocessed *Toxoplasma* ROP1 is effectively targeted and secreted into the nascent parasitophorous vacuole. Mol. Biochem. Parasitol. 125, 189–193.

Bradley, P.J., Li, N., Boothroyd, J.C., 2004. A GFP-based motif-trap reveals a novel mechanism of targeting for the *Toxoplasma* ROP4 protein. Mol. Biochem. Parasitol. 137, 111–120.

Bradley, P.J., Ward, C., Cheng, S.J., Alexander, D.L., Coller, S., Coombs, G.H., Dunn, J.D., Ferguson, D.J., Sanderson, S.J., Wastling, J.M., Boothroyd, J.C., 2005. Proteomic analysis of rhoptry organelles reveals many novel constituents for host–parasite interactions in *Toxoplasma gondii*. J. Biol. Chem. 280, 34245–34258.

Burg, J.L., Perelman, D., Kasper, L.H., Ware, P.L., Boothroyd, J.C., 1988. Molecular analysis of the gene encoding the major surface antigen of *Toxoplasma gondii*. J. Immunol. 141, 3584–3591.

Butcher, B.A., Greene, R.I., Henry, S.C., Annecharico, K.L., Weinberg, J.B., Denkers, E.Y., Sher, A., Taylor, G.A., 2005. p47 GTPases regulate *Toxoplasma gondii* survival in activated macrophages. Infect. Immun. 73, 3278–3286.

Carey, K.L., Jongco, A.M., Kim, K., Ward, G.E., 2004. The *Toxoplasma gondii* rhoptry protein ROP4 is secreted into the parasitophorous vacuole and becomes phosphorylated in infected cells. Eukaryot. Cell 3, 1320–1330.

Dunn, J.D., Ravindran, S., Kim, S.-K., Boothroyd, J.C., 2008. The *Toxoplasma gondii* dense granule protein GRA7 is phosphorylated upon invasion and forms an unexpected association with the rhoptry proteins ROP2 and ROP4. Infect. Immun. 76, 5853–5861.

Fentress, S.J., Behnke, M.S., Dunay, I.R., Mashayekhi, M., Rommereim, L.M., Fox, B.A., Bzik, D.J., Taylor, G.A., Turk, B.E., Lichti, C.F., Townsend, R.R., Qiu, W., Hui, R., Beatty, W.L., Sibley, L.D., 2010. Phosphorylation of immunity-related GTPases by a *Toxoplasma gondii*-secreted kinase promotes macrophage survival and virulence. Cell Host Microbe 8, 484–495.

Fentress, S.J., Steinfeldt, T., Howard, J.C., Sibley, L.D., 2012. The arginine-rich N-terminal domain of ROP18 is necessary for vacuole targeting and virulence of *Toxoplasma gondii*. Cell. Microbiol. 14, 1921–1933.

Fleckenstein, M.C., Reese, M.L., Könen-Waisman, S., Boothroyd, J.C., Howard, J.C., Steinfeldt, T., 2012. A *Toxoplasma gondii* pseudokinase inhibits host IRG resistance proteins. PLoS Biol. 10, e1001358.

Fox, B.A., Falla, A., Rommereim, L.M., Tomita, T., Gigley, J.P., Mercier, C., Cesbron-Delauw, M.-F., Weiss, L.M., Bzik, D.J., 2011. Type II *Toxoplasma gondii* KU80 knockout strains enable functional analysis of genes required for cyst development and latent infection. Eukaryot. Cell 10, 1193–1206.

Fritz, H.M., Buchholz, K.R., Chen, X., Durbin-Johnson, B., Rocke, D.M., Conrad, P.A., Boothroyd, J.C., 2012. Transcriptomic analysis of *Toxoplasma* development reveals many novel functions and structures specific to sporozoites and oocysts. PLoS ONE 7, e29998.

Gilbert, L.A., Ravindran, S., Turetzky, J.M., Boothroyd, J.C., Bradley, P.J., 2007. *Toxoplasma gondii* targets a protein phosphatase 2C to the nuclei of infected host cells. Eukaryot. Cell 6, 73–83.

Hajagos, B.E., Turetzky, J.M., Peng, E.D., Cheng, S.J., Ryan, C.M., Souda, P., Whitelegge, J.P., Lebrun, M., Dubremetz, J.-F., Bradley, P.J., 2011. Molecular dissection of novel trafficking and processing of the *Toxoplasma gondii* rhoptry metalloprotease toxolysin-1. Traffic 13, 292–304.

Hajj, El.H., Demey, E., Poncet, J., Lebrun, M., Wu, B., Galéotti, N., Fourmaux, M.N., Mercereau-Puijalon, O., Vial, H., Labesse, G., Dubremetz, J.-F., 2006a. The ROP2 family of *Toxoplasma gondii* rhoptry proteins: proteomic and genomic characterization and molecular modeling. Proteomics 6, 5773–5784.

Hajj, El.H., Lebrun, M., Fourmaux, M.N., Vial, H., Dubremetz, J.-F., 2006b. Characterization, biosynthesis and fate of ROP7, a ROP2 related rhoptry protein of *Toxoplasma gondii*. Mol. Biochem. Parasitol. 146, 98–100.

Hajj, El.H., Lebrun, M., Arold, S.T., Vial, H., Labesse, G., Dubremetz, J.-F., 2007. ROP18 is a rhoptry kinase controlling the intracellular proliferation of *Toxoplasma gondii*. PLoS Pathog. 3, e14.

Hoppe, H.C., Ngô, H.M., Yang, M., Joiner, K.A., 2000. Targeting to rhoptry organelles of *Toxoplasma gondii* involves evolutionarily conserved mechanisms. Nat. Cell Biol. 2, 449–456.

Huynh, M.-H., Carruthers, V.B., 2009. Tagging of endogenous genes in a *Toxoplasma gondii* strain lacking Ku80. Eukaryot. Cell 8, 530–539.

Joiner, K.A., Roos, D.S., 2002. Secretory traffic in the eukaryotic parasite *Toxoplasma gondii*: less is more. J. Cell Biol. 157, 557–563.

Karasov, A.O., Boothroyd, J.C., Arrizabalaga, G., 2005. Identification and disruption of a rhoptry-localized homologue of sodium hydrogen exchangers in *Toxoplasma gondii*. Int. J. Parasitol. 35, 285–291.

Kawase, O., Nishikawa, Y., Bannai, H., Zhang, H., Zhang, G., Jin, S., Lee, E.-G., Xuan, X., 2007. Proteomic analysis of calcium-dependent secretion in*Toxoplasma gondii*. Proteomics 7, 3718–3725.

Kissinger, J.C., Gajria, B., Li, L., Paulsen, I.T., Roos, D.S., 2003. ToxoDB: accessing the *Toxoplasma gondii* genome. Nucleic Acids Res. 31, 234–236.

Kosugi, S., Hasebe, M., Tomita, M., Yanagawa, H., 2009. Systematic identification of cell cycle-dependent yeast nucleocytoplasmic shuttling proteins by prediction of composite motifs. Proc. Natl. Acad. Sci. USA 106, 10171–10176.

Lamarque, M.H., Papoin, J., Finizio, A.-L., Lentini, G., Pfaff, A.W., Candolfi, E., Dubremetz, J.-F., Lebrun, M., 2012. Identification of a new rhoptry neck complex RON9/RON10 in the apicomplexa parasite *Toxoplasma gondii*. PLoS ONE 7, e32457.

Lodoen, M.B., Gerke, C., Boothroyd, J.C., 2010. A highly sensitive FRET-based approach reveals secretion of the actin-binding protein toxofilin during *Toxoplasma gondii* infection. Cell. Microbiol. 12, 55–66.

Marugán-Hernández, V., Álvarez-García, G., Tomley, F., Hemphill, A., Regidor-Cerrillo, J., Ortega-Mora, L.M., 2011. Identification of novel rhoptry proteins in *Neospora caninum* by LC/MS–MS analysis of subcellular fractions. J. Proteomics 74, 629–642.

Miller, S.A., Thathy, V., Ajioka, J.W., Blackman, M.J., Kim, K., 2003. TgSUB2 is a *Toxoplasma gondii* rhoptry organelle processing proteinase. Mol. Microbiol. 49, 883–894.

Minot, S., Melo, M.B., Li, F., Lu, D., Niedelman, W., Levine, S.S., Saeij, J.P.J., 2012. Admixture and recombination among *Toxoplasma gondii* lineages explain global genome diversity. Proc. Natl. Acad. Sci. USA 109, 13458–13463.

Montoya, J.G., Liesenfeld, O., 2004. Toxoplasmosis. Lancet 363, 1965–1976.

Niedelman, W., Gold, D.A., Rosowski, E.E., Sprokholt, J.K., Lim, D., Farid Arenas, A., Melo, M.B., Spooner, E., Yaffe, M.B., Saeij, J.P.J., 2012. The rhoptry proteins ROP18 and ROP5 mediate *Toxoplasma gondii* evasion of the murine, but not the human, interferon-gamma response. PLoS Pathog. 8, e1002784.

Oakes, R.D., Kurian, D., Bromley, E., Ward, C., Lal, K., Blake, D.P., Reid, A.J., Pain, A., Sinden, R.E., Wastling, J.M., Tomley, F.M., 2013. The rhoptry proteome of *Eimeria tenella* sporozoites. Int. J. Parasitol. 43, 181–188.

Ong, Y.-C., Reese, M.L., Boothroyd, J.C., 2010. *Toxoplasma* rhoptry protein 16 (ROP16) subverts host function by direct tyrosine phosphorylation of STAT6. J. Biol. Chem. 285, 28731–28740.

Ossorio, P.N., Schwartzman, J.D., Boothroyd, J.C., 1992. A *Toxoplasma gondii* rhoptry protein associated with host cell penetration has unusual charge asymmetry. Mol. Biochem. Parasitol. 50, 1–15.

Peixoto, L., Chen, F., Harb, O.S., Davis, P.H., Beiting, D.P., Brownback, C.S., Ouloguem, D., Roos, D.S., 2010. Integrative genomic approaches highlight a family of parasite-specific kinases that regulate host responses. Cell Host Microbe 8, 208–218.

Proellocks, N.I., Kats, L.M., Sheffield, D.A., Hanssen, E., Black, C.G., Waller, K.L., Coppel, R.L., 2009. Characterisation of PfRON6, a *Plasmodium falciparum* rhoptry neck protein with a novel cysteine-rich domain. Int. J. Parasitol. 39, 683–692.

Reese, M.L., Boothroyd, J.C., 2009. A helical membrane-binding domain targets the *Toxoplasma* ROP2 family to the parasitophorous vacuole. Traffic 10, 1458–1470.

Reid, A.J., Vermont, S.J., Cotton, J.A., Harris, D., Hill-Cawthorne, G.A., Könen-Waisman, S., Latham, S.M., Mourier, T., Norton, R., Quail, M.A., Sanders, M., Shanmugam, D., Sohal, A., Wasmuth, J.D., Brunk, B., Grigg, M.E., Howard, J.C., Parkinson, J., Roos, D.S., Trees, A.J., Berriman, M., Pain, A., Wastling, J.M., 2012. Comparative genomics of the apicomplexan parasites *Toxoplasma gondii* and *Neospora caninum*: Coccidia differing in host range and transmission strategy. PLoS Pathog. 8, e1002567.

Rosowski, E.E., Lu, D., Julien, L., Rodda, L., Gaiser, R.A., Jensen, K.D.C., Saeij, J.P.J., 2011. Strain-specific activation of the NF-kappaB pathway by GRA15, a novel *Toxoplasma gondii* dense granule protein. J. Exp. Med. 208, 195–212.

Sadak, A., Taghy, Z., Fortier, B., Dubremetz, J.F., 1988. Characterization of a family of rhoptry proteins of *Toxoplasma gondii*. Mol. Biochem. Parasitol. 29, 203–211.

Saeij, J.P.J., Boyle, J.P., Coller, S., Taylor, S., Sibley, L.D., Brooke-Powell, E.T., Ajioka, J.W., Boothroyd, J.C., 2006. Polymorphic secreted kinases are key virulence factors in toxoplasmosis. Science 314, 1780–1783.

Saeij, J.P.J., Coller, S., Boyle, J.P., Jerome, M.E., White, M.W., Boothroyd, J.C., 2007. *Toxoplasma* co-opts host gene expression by injection of a polymorphic kinase homologue. Nature 445, 324–327.

Scallan, E., Hoekstra, R.M., Angulo, F.J., Tauxe, R.V., Widdowson, M.-A., Roy, S.L., Jones, J.L., Griffin, P.M., 2011. Foodborne illness acquired in the United States–major pathogens. Emerging Infect. Dis. 17, 7–15.

Schwarz, J.A., Fouts, A.E., Cummings, C.A., Ferguson, D.J.P., Boothroyd, J.C., 2005. A novel rhoptry protein in *Toxoplasma gondii* bradyzoites and merozoites. Mol. Biochem. Parasitol. 144, 159–166.

Sohn, W.M.W., Nam, H.W.H., 1999. Western blot analysis of stray cat sera against *Toxoplasma gondii* and the diagnostic availability of monoclonal antibodies in sandwich-ELISA. Korean J. Parasitol. 37, 249–256.

Steinfeldt, T., Könen-Waisman, S., Tong, L., Pawlowski, N., Lamkemeyer, T., Sibley, L.D., Hunn, J.P., Howard, J.C., 2010. Phosphorylation of mouse immunity-related GTPase (IRG) resistance proteins is an evasion strategy for virulent *Toxoplasma gondii*. PLoS Biol. 8, e1000576.

Straub, K.W., Cheng, S.J., Sohn, C.S., Bradley, P.J., 2009. Novel components of the Apicomplexan moving junction reveal conserved and coccidia-restricted elements. Cell. Microbiol. 11, 590–603.

Straub, K.W., Peng, E.D., Hajagos, B.E., Tyler, J.S., Bradley, P.J., 2011. The moving junction protein RON8 facilitates firm attachment and host cell invasion in *Toxoplasma gondii*. PLoS Pathog. 7, e1002007.

Suzuki, Y., Orellana, M., Schreiber, R., Remington, J., 1988. Interferon-gamma: the major mediator of resistance against *Toxoplasma gondii*. Science 240, 516–518.

Taylor, S., Barragan, A., Su, C., Fux, B., Fentress, S.J., Tang, K., Beatty, W.L., Hajj, H.E., Jerome, M., Behnke, M.S., White, M., Wootton, J.C., Sibley, L.D., 2006. A secreted

serine–threonine kinase determines virulence in the eukaryotic pathogen *Toxoplasma gondii*. Science 314, 1776–1780.
Turetzky, J.M., Chu, D.K., Hajagos, B.E., Bradley, P.J., 2010. Processing and secretion of ROP13: a unique *Toxoplasma* effector protein. Int. J. Parasitol. 40, 1037–1044.
Yamamoto, M., Standley, D.M., Takashima, S., Saiga, H., Okuyama, M., Kayama, H., Kubo, E., Ito, H., Takaura, M., Matsuda, T., Soldati-Favre, D., Takeda, K., 2009. A single polymorphic amino acid on *Toxoplasma gondii* kinase ROP16 determines the direct and strain-specific activation of Stat3. J. Exp. Med. 206, 2747–2760.
Zhao, Y.O., Rohde, C., Lilue, J.T., Könen-Waisman, S., Khaminets, A., Hunn, J.P., Howard, J.C., 2009. *Toxoplasma gondii* and the immunity-related GTPase (IRG) resistance system in mice: a review. Mem. Inst. Oswaldo Cruz 104, 234–240.